A parallel transmit spectral-spatial pulse design method for ultra-high field MRS combining LSQR and optimal control based optimization

Tingting Shao[1], Yun Zhang[2], Nikolai Avdievich[1], Steffen Glaser[2], and Anke Henning[1,3]

[1]*Max Planck Institute for Biological Cybernetics, Tübingen, Baden-Württemberg, Germany,* [2]*Department of Chemistry, Technical University of Munich, Garching, Germany,* [3]*Institute for Biomedical Engineering, UZH and ETH Zurich, Zurich, Switzerland*

Introduction

Ultra high field MRI benefits ^{1}H magnetic resonance spectroscopy (MRS) applications by offering increased chemical shift dispersion, improved SNR and reduced J-coupling, but also raises technical challenges such as shortened T_2 and T_2* relaxation times, severe chemical shift displacement artifacts and signal disuniformity due to high spatial B_1^+ field inhomogeneity. **In this work**, a parallel transmission based pulse design method that combines subspace preconditioned least squares optimization (LSQR) [1] and optimal control (OC) [2] approaches is proposed to achieve spectral-spatial pulses (SPSP) that tackle aforementioned technical challenges in ultra-high field ^{1}H MRS.

Methodology

B1 map and basic settings The B_1+ & B_0 field maps [3] were acquired with a home-built 8-channel TxRx array head coil [4] and a spherical spectroscopy phantom filled with an aqueous solution of acetate and lactate on a 9.4T Magnetom SIEMENS scanner (SIEMENS Healthcare, Erlangen, Germany), using a pre-conditioning RF pulse with TurboFLASH readout [3], as shown in Fig 1(a). The desired excitation pattern is a uniform rectangle (5cm*7.5cm, blurred by convolution with a Gaussian kernel of FWHM = 1.2 cm) in a slice of 22cm FOV, as shown in Fig 1(b), and a uniform band along the spectral axis, with 2kHz (or 4ppm) bandwidth that is sufficient to cover the spectral range of interest at 9.4 Tesla (1.6kHz).

RF pulse design method The 2D parallel transmit RF pulses (acceleration factor: 2, channels: 8) are designed based on the small-tip-angle (STA) approach [5], a novel iterative design approach and a spiral trajectory.

Subspace preconditioned LSQR [3] and quasi-Newton based optimal control (OC) [4] optimization approaches were combined in the iterative design process. It has been observed that the LSQR method performs well for 2D spatial pulses, but has difficulty to converge in the SPSP case. In contrast the OC method converges well in the SPSP case but is prone to reach local minima. Therefore we combine both methods such that a spatially selective excitation pulse is designed first using the LSQR method. Afterwards the result is used as an initial guess for the OC method for further optimization into an SPSP pulse.

Spinor-domain based Bloch simulations were implemented to produce the excitation and saturation profiles of the designed pulses. Both pulse calculation and excitation profile simulation were performed using self-written scripts in MATLAB (2012B, The Mathworks, Natick, USA). Both excitation (flip angle 35°) and saturation (flip angle 90°) pulses with both durations of 4.10 ms and maximum B_1^+ amplitude of 34.5 uT have been designed.

Results and discussion

Fig 1 shows the B_1^+ maps of all individual 8 channels that served as input for the parallel transmit pulse design and approached a maximum B_1^+ value of 34.5 uT the highest possible voltage of 150V per channel was applied. The pulse design algorithm also considered a B_0 inhomogeneity correction based on the displayed B_0 map. Fig 2-5 show the spectral-spatial saturation and excitation profiles of 1) a spatially selective excitation pulse designed using the LSQR method, 2) an SPSP saturation pulse designed using the OC method only, 3) SPSP saturation and 4) excitation pulses designed using LSQR and OC methods in a combined manner. All the pulses share the same spiral k-space trajectory. The 1) spatially selective excitation pulse is used as an initial guess in the calculations of the pulses shown in 3) and 4). Table 1 shows the maximum RF amplitude and power integrations those pulses require.

By comparison of Fig 3 and 4, it can be seen that the use of the initial guess calculated by the LSQR method helps to direct the OC method to an optimized global minimum instead of sticking in the local minimum with bad performance. It can be seen from Fig 4 and 5 that the excitation profile of the designed excitation pulse has a wider transition band than the saturation pulses, which is due to the more demanding optimization problem in case of excitation pulses in comparison to saturation pulses in case the same pulse duration is chosen.

The simulation results show promising performance of the proposed combination of LSQR and OC optimization approaches to parallel transmit SPSP pulse design. Similar excitation and saturation pulses may be used in future for FID MRSI at 9.4T [6,7], which could lead to a homogeneous spatial-spectral excitation profile and better lipid suppression at reduced SAR deposition in comparison to spatially selective outer volume suppression.

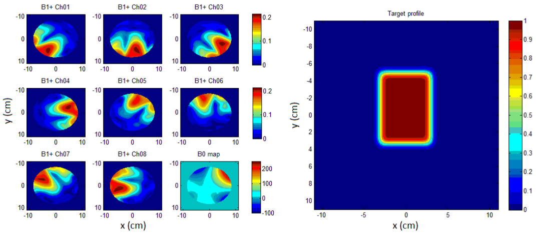

(a) (b)

Fig 1 (a) B_1^+ maps of all 8 channels (range in 0 ~ 0.2 uT per voltage) and B_0 map (range in -100 ~ 250 Hz). (b) Spatially desired excitation / saturation profile.

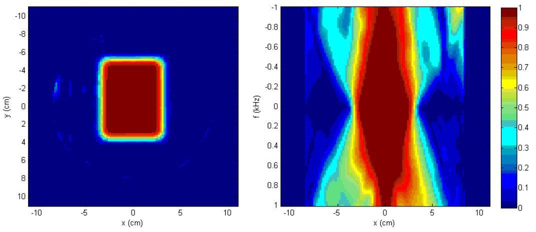

(a) (b)

Fig 2 Transverse (a) and cut-away (b) views of the spectral-spatial saturation profile (|Mxy|) of a spatially selective excitation pulse designed by the LSQR method.

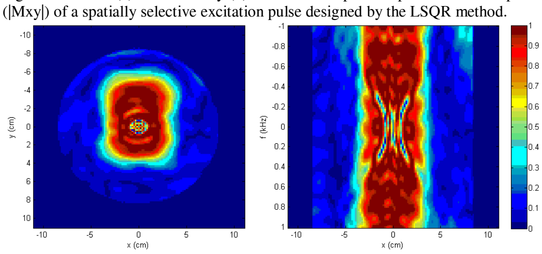

(a) (b)

Fig 3 Transverse (a) and cut-away (b) views of the spectral-spatial saturation profile (|Mxy|) of a saturation pulse designed using the OC method only.

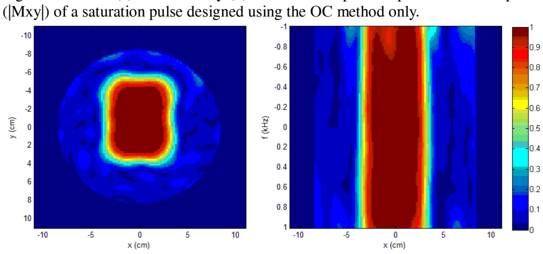

(a) (b)

Fig 4 Transverse (a) and cut-away (b) views of the spectral-spatial saturation profile (|Mxy|) of a saturation pulse designed using the LSQR and OC methods in a combined manner.

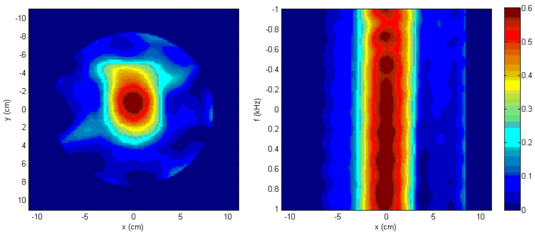

(a) (b)

Fig 5 Transverse (a) and cut-away (b) views of the spectral-spatial excitation profile (My) of an excitation pulse designed using the LSQR and OC methods in a combined manner.

Table 1 Maximum RF amplitude & RF integration

Pulse index	Fig 2	Fig 3	Fig 4	Fig 5
|RF| max (uT)	14.4	24.5	30.9	31.8
RF Integration ($uT^2 \cdot ms$)	197.2	414.9	421.3	137.1

Reference

[1] Jacobsen et al., BIT Numerical Mathematics 43: 975–989 (2003). [2] de Fouquieres et al., JMR 212, 412-417 (2011). [3] Chung et al., MRM 64(2):439-446 (2010). [4] Avdievich NI et al. ISMRM and ESMRMB: 622 (2014). [5] Grissom et al., MRM 53:620-629 (2006). [6] Henning et al. NMR Biomed Aug; 22(7):683-96 (2009). [7] Chadzynski GL et al. ISMRM and ESMRMB: 2904 (2014).